

Defect mechanism of photoinduced superconductivity in $\text{YBa}_2\text{Cu}_3\text{O}_{6+x}$

J. F. Federici, D. Chew, B. Welker, W. Savin, J. Gutierrez-Solana, and T. Fink
Department of Physics, New Jersey Institute of Technology, Newark, New Jersey 07102

W. Wilber

Physical Science Directorate, Army Research Laboratory, Fort Monmouth, New Jersey 07703-5601

(Received 17 May 1995; revised manuscript received 27 July 1995)

Although persistent photoconductivity and photoinduced superconductivity have been experimentally observed in oxygen-deficient and superconducting $\text{YBa}_2\text{Cu}_3\text{O}_{6+x}$, the mechanism which is responsible for these effects is still under debate. The possibility of a defect related mechanism in laser-deposited thin films of $\text{YBa}_2\text{Cu}_3\text{O}_{6+x}$ is studied using four-point resistivity and photoluminescence techniques. It is found that there is a correlation between the photoluminescence spectrum and the wavelength dependence of the photoinduced conductivity. Peaks in the luminescence spectrum change intensity upon initiation of the photoinduced state. These results support an oxygen vacancy defect model of photoinduced persistent conductivity and superconductivity in which the oxygen vacancies act as weakly luminescent F -centers under illumination.

When a sufficiently intense light pulse whose energy exceeds the superconducting energy gap interacts with a superconductor, the light pulse interferes with the Cooper paired electrons (e.g., heats the sample above T_c , or directly dissociates paired electrons) and destroys the superconductivity.¹ However, for high-transition-temperature (high- T_c) copper oxide superconductors, experimental evidence²⁻⁵ indicates that the interaction of the light pulse with the superconductor can *enhance* the copper oxide's superconducting properties (i.e., transition temperature T_c , conductivity, and diamagnetism). The relevant physical mechanism for this persistent photoconductivity (PPC) and photoinduced superconductivity (PISC) is not well understood. This paper addresses the possibility of a defect mechanism of PPC and PISC in $\text{YBa}_2\text{Cu}_3\text{O}_{6+x}$.

Conceptually, PPC and PISC can be viewed as "photodoping" a high- T_c parent compound analogous to chemical doping of a material from an insulator to metal. In the case of $\text{YBa}_2\text{Cu}_3\text{O}_{6+x}$, this photodoping is analogous to increasing the oxygen content from $\text{YBa}_2\text{Cu}_3\text{O}_6$ to $\text{YBa}_2\text{Cu}_3\text{O}_{7-\delta}$. Subsequent to photoexciting a nonsuperconducting, oxygen-deficient $\text{YBa}_2\text{Cu}_3\text{O}_{6+x}$ film, one photogenerated charge species (electrons) is trapped while the other species (holes) contributes to the transient conductivity. If the transient carrier density were high enough, a transition from insulator to metal would occur. Presumably, if the charge carriers were able to form Cooper pairs, a superconducting phase would form. The effect decays as photogenerated holes and electrons recombine.

Various groups have studied the PPC-PISC effect using electrical resistivity, Hall effect, photoconductivity techniques, diamagnetism measurements, and x-ray scattering.²⁻⁶ Several possible mechanisms have been proposed to explain PISC: (1) intrinsic defects and/or (2) polaronic type excitations which trap photogenerated electrons and prevent recombination of electrons and holes, (3) photoinduced diffusion of oxygen, (4) photoinduced charge transfer in the CuO_2 planes, and (5) electronic phase separation.^{5,7}

Kudinov *et al.*^{8,9} established the existence of a photoinduced transition to a metallic state and photoinduced superconductivity in $\text{YBa}_2\text{Cu}_3\text{O}_{6+x}$ (YBCO) films. In addition, a persistent diamagnetic moment of the photoinduced state, a condition indicative of a superconducting phase, was observed. The observed PPC persisted for hours at room temperature. The relaxation of PPC can be described² by a thermally activated process with an energy barrier of about 1 eV. The authors suggested that the long lifetime could be due to the formation of a long-lived localized structural distortion around the photogenerated electron (polaronic structure). In recent work, Bud'ko *et al.*³ and Kudinov *et al.*² used a variable-wavelength excitation source to study the spectral dependence of the PPC response. The observed PPC efficiency curve was numerically fit to six Lorentzian lines throughout the visible range.¹⁰ If a Mott-Hubbard model is used, the six peaks of the PPC spectra can be assigned to electron transitions in the CuO_2 planes corresponding to photoinduced charge transfer between the conduction band and the upper Hubbard unoccupied subband. As will be described in this paper, we attribute these spectral peaks to CuO chain excitations in which electrons are trapped at oxygen vacancies (F centers).

It is well established that the T_c of quenched YBCO samples slowly increases over time.^{11,12} In the slow annealing process which leads to an increased T_c , the sample composition is not altered (oxygen is neither added nor removed), but the location (ordering) of the oxygen in the lattice changes. In these samples, oxygen reordering during annealing induces a transfer of holes to the CuO_2 planes and a commensurate increase in T_c . In the proposed photoassisted oxygen ordering mechanism, illumination of semiconducting or reduced T_c material induces the required reordering of oxygen for charge transfer of holes to the CuO_2 planes and a superconducting transition. The PISC effect decays as the oxygen thermally diffuses back to its initial configuration. However, Hall and lattice parameter measurements^{13,6,4} strongly suggest that PISC is not due to oxygen reordering. Nieva *et al.*⁴ conclude that oxygen ordering may be ruled out

TABLE I. Characteristic photoluminescence peaks in $\text{YBa}_2\text{Cu}_3\text{O}_{6+x}$. TSL means thermally stimulated luminescence.

| Reference | Technique | Luminescence peaks (eV) | Activation energy |
|-----------|----------------|----------------------------|----------------------------------|
| 15 | x-ray TSL | 3.65 2.9 | 0.16, 0.42 eV |
| 16 | x-ray TSL | 1.88, 3.63 | 0.429 eV 0.265 eV 0.290 eV |
| 17, 18 | cathodo | 3.355 | 0.024 eV |
| 19 | cathodo | 3.36, 2.9 3.6, 2.9, 2.4 | |
| 20, 21 | photo, cathodo | 2.9 | |
| 22 | cathodo | 3.36, 3.31 | |
| 23 | cathodo | 3.36, 3.31 | |
| 24 | cathodo | 2.75, 1.91 | |
| 25 | cathodo | 3.65, 2.58, 2.7 | |

as a PISC mechanism because the electrical resistivity and Hall coefficient evolve in opposite ways for PISC samples and quenched samples. Likewise, the results of Hasen *et al.*¹³ and Lederman *et al.*⁶ show that the oxygen diffusion model is incorrect: The model incorrectly predicts that the magnitude of the PPC effect should diminish for low oxygen concentrations.

It has been suggested that defects, most likely oxygen vacancies in the case of YBCO,^{14,2,13} potentially play an important role in the PPC-PISC mechanism. In this model, defects trap photogenerated electrons so that electron-hole recombination cannot occur, thereby allowing photogenerated holes to contribute to the carrier density. Clearly, if defects are important to PISC, then the luminescence spectra of high- T_c superconductors is one tool which may provide insight into the nature and dynamics of the defects. Table I summarizes previous luminescence studies of superconducting YBCO subsequent to excitation by electron beams (cathodoluminescence), synchrotron radiation, and x rays. All of the studies show a weak luminescence of the superconductor. As seen from Table I, the most common luminescence peaks are at 1.9, 2.4, 2.9, 3.35, and 3.6 eV with corresponding thermal activation energies in the 0.2–0.5 eV range. These activation energies are the same order of magnitude as measurements of the thermal activation energy (0.935 eV) for the decay of PISC.² Some features, such as the 1.88-eV peak, are narrow. Other features, such the 2.4-eV peak, are broad. From luminescence measurements, the density of defects were estimated by Roth *et al.*¹⁵ to be at least 1 of every 10^4 lattice cells assuming unity quantum yield. If the quantum yield is closer to the 10^{-3} – 10^{-4} as estimated by Lushchik *et al.*,¹⁷ this suggests that *the density of defects may approach one defect per unit cell.*

In this paper, photoconductivity and photoluminescence measurements on insulating, suppressed T_c , and fully superconducting $\text{YBa}_2\text{Cu}_3\text{O}_{6+x}$ films are used to study the feasibility of a defect mechanism for PPC and PISC. $\text{YBa}_2\text{Cu}_3\text{O}_{6+x}$ samples are fabricated using pulsed laser deposition. The deposition system consists of a KrF excimer

laser and a turbo-pumped vacuum chamber containing the target and the heated substrate holder. Under typical growth conditions, the laser is operated at 10 Hz at 300 mJ/pulse and is focused to 1–2 J/cm² at the target. The oxygen pressure during deposition is typically held in the 100–200 mTorr range and the substrate temperature is about 800 °C. The substrate is fastened to an Inconel heater block that is heated optically from behind. After deposition the samples are allowed to cool in 1/2 atm of oxygen. The laser deposition on LaAlO_3 substrates yields films which exhibit transition temperatures of approximately 90 K and transition widths of less than 1/2 °.

The 2500-Å-thick $\text{YBa}_2\text{Cu}_3\text{O}_{7-\delta}$ films produced in this manner are fully oxygenated, providing a consistent starting point for de-oxygenation through annealing. Gold contacts are evaporated onto the thin films and annealed prior to oxygen annealing. The contacts are arranged near the edges of the film to permit laser irradiation of the film and simultaneous electrical and optical measurements. The samples are de-oxygenated in an oven with a controlled flow of oxygen over the sample during heating and cooling. For convenience, the superconducting films are mounted in a ceramic package, to which is connected (via copper wire) an external ohmmeter. The meter allows real-time monitoring of the film resistance. The oxygen flow (0.7 l/min) ensures that the sample remains fully oxygenated while being brought up to 500 °C. When the target temperature is reached, the heater is turned off and the sample is allowed to cool. During this cooling process, the rate of resistance change ($\Omega/^\circ\text{C}$) is monitored to determine approximately where the final resistance will settle. Accordingly, the oxygen flow through the chamber can be adjusted to vary the rate of de-oxygenation and control the observed rate of resistance change. The precise oxygen content of the finished sample can then be determined by x-ray diffraction using published results of lattice parameter vs oxygen content.

The de-oxygenated films are mounted in a ceramic dual in-line package with the contacts wire bonded to the gold contacts on the sample. The package is inserted into a liquid-nitrogen-cooled optical cryostat. The film resistance is measured using standard four-point resistivity techniques while the photoluminescence is measured using a 0.25-m scanning grating monochromator (spectral resolution 1 nm) and a photomultiplier detector. The photoluminescence spectrum is measured by mechanically chopping a low-intensity laser beam (30 mW, 476.2 nm, 4 mm spot size) and using phase-sensitive detection to measure the photoluminescence spectrum as the monochromator is scanned. A yellow glass filter is placed in front of the monochromator entrance slit to reject stray laser light. The monochromator, photomultiplier detector, and four-point resistivity electronics are interfaced to an automated data-acquisition system.

The room-temperature and 77-K (unilluminated) photoluminescence spectra of an insulating $\text{YBa}_2\text{Cu}_3\text{O}_{6.4}$ film are shown in Fig. 1. The excitation light for photoluminescence is kept at 30 mW to minimize the changes in photoinduced conductivity during the luminescence data acquisition. There are narrow luminescent peaks at 1.88 and 2.03 eV while a broad feature near 2.4 eV appears upon cooling. Comparing the 77-K (unilluminated) luminescence spectra of the insulating $\text{O}_{6.4}$ film to those of the suppressed T_c $\text{O}_{6.6}$ and full

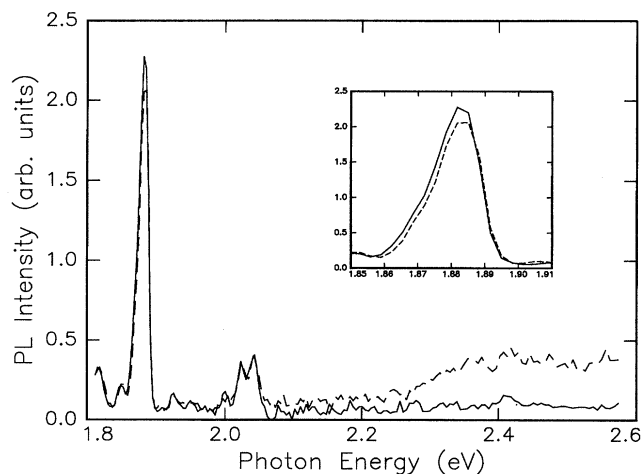


FIG. 1. Photoluminescence spectrum of $\text{YBa}_2\text{Cu}_3\text{O}_{6.4}$ 2500-Å film at room temperature (solid line) and at 77 K (dashed line). Inset: 1.88-eV peak on an expanded scale. As the temperature is reduced to 77 K, there is a small decrease in luminescence at 1.88 eV and a broad increase near 2.4 eV. In all data shown, the excitation source for photoluminescence is 30 mW of 476.2-nm light.

superconducting $\text{O}_{7-\delta}$ films shows that the intensity of the 1.88-eV peak decreases by roughly a factor of 100 with increasing oxygen content. This observed decrease in 1.88-eV luminescence with increasing oxygen content (or equivalently a decreasing population of oxygen chain vacancies) has been noted in previous luminescence studies. The ratio of the 1.88-eV to 2.4-eV intensity peaks also changed as the oxygen content increased. For the insulating films, this ratio was $\text{PL}_{1.88}/\text{PL}_{2.4}=10$, while for the $\text{O}_{6.6}$ and $\text{O}_{7-\delta}$ samples, the ratio was about 1 and 0.2, respectively.

In previous $\text{YBa}_2\text{Cu}_3\text{O}_{6+x}$ luminescence studies, Cooke *et al.*^{26,15} used an analogy with simpler oxide systems such as Al_2O_3 , MgO , and BeO to suggest that F centers (two electrons trapped at an oxygen vacancy) and F^+ centers (one electron trapped at an oxygen vacancy) are responsible for the two peaks (1.88 and 3.63 eV) which Cooke *et al.* observed in luminescence spectra of YBCO superconductors. In following the interpretation of Cooke *et al.*, the luminescence at 1.88 eV in our defect model of PPC and PISC is a direct measure of the oxygen chain vacancy: As the number of oxygen vacancies decreases, the luminescence at 1.88 eV decreases. By correlating photoluminescence with electrical measurements of PISC, it will be apparent if these hypothesized luminescent defects are a fundamental component of the PISC mechanism.

Upon illumination with 4 W of argon-ion laser light and the initiation of the persistent photoconductivity state, both the resistance and luminescence spectra of the $\text{YBa}_2\text{Cu}_3\text{O}_{6+x}$ films change. Figure 2(a) shows a typical resistance versus temperature curve of an insulating $\text{YBa}_2\text{Cu}_3\text{O}_{6.4}$ film before and after 1 h of illumination (4 W, all lines) from an argon-ion laser. During illumination, the sample is immersed in liquid nitrogen to maintain it at a constant temperature. This ensures that any observed changes in photoluminescent intensity are due to the photoinduced state and are not due to temperature-induced changes in the defects' luminescent properties. The illuminated sample's resistivity returns to its

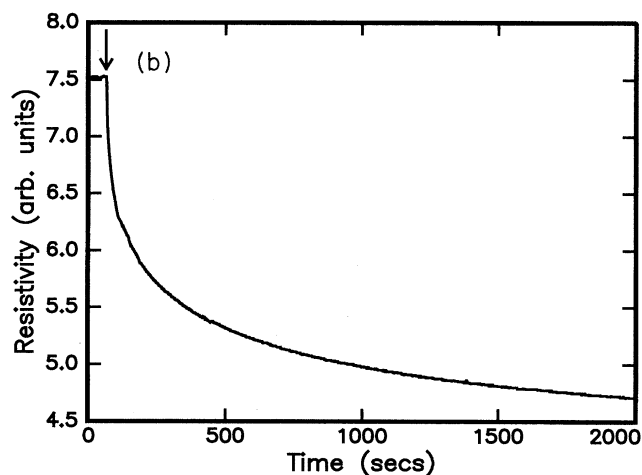
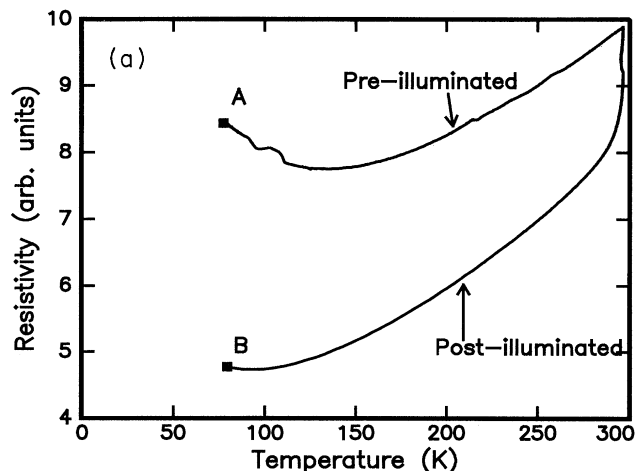


FIG. 2. (a) Resistance versus temperature curve of $\text{YBa}_2\text{Cu}_3\text{O}_{6.4}$ 2500-Å film before illumination (upper curve). Lower curve shows resistance versus temperature of same film after 1 h illumination with 4-W argon-ion laser light while sample is immersed in liquid nitrogen. (b) Time dependence of resistance during illumination of $\text{YBa}_2\text{Cu}_3\text{O}_{6.4}$ sample immersed in liquid nitrogen. The arrow indicates when the sample is exposed to laser light.

unilluminated value after approximately 33 h at room temperature. Figure 2(b) shows the electrical resistance of the film at 77 K as a function of time during the 4-W illumination.

The 77-K photoluminescence spectra at points A and B of Fig. 2(a) (before illumination and immediately after illumination) are shown in Fig. 3. After 1 h of illumination, there is a drop ($\sim 15\%$) in the luminescent intensity at 1.88 eV and an increase at 2.4 eV while the photoluminescent intensity at 2.03 eV remained constant. Figure 4 shows the time dependence of the resistivity and 1.88-eV luminescence during the 4-W illumination of the $\text{O}_{6.6}$ sample. The correlation between the photoinduced conductivity and luminescence strongly suggests that the luminescence at 1.88 eV is indicative of the PPC-PISC state.

The change in luminescence at 1.88 eV under 4-W illumination is observed to be consistent with its assignment as a measure of the number of available oxygen vacancies.

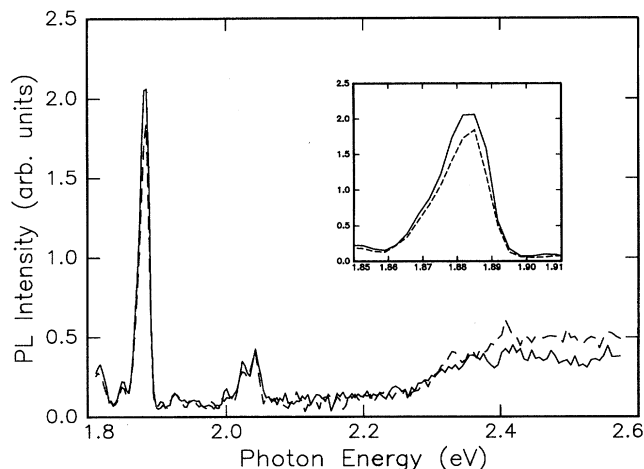


FIG. 3. Photoluminescence spectrum of $\text{YBa}_2\text{Cu}_3\text{O}_{6.4}$ 2500-Å film immersed in liquid nitrogen before [solid line, point A of Fig. 2(a)] and after [dashed line, point B of Fig. 2(a)] 1 h illumination with 4 W of laser light. Inset shows the 1.88-eV peak on an expanded scale. Upon photoexcitation, the luminescence at 1.88 eV decreases while the luminescence near 2.4 eV increases.

While the insulating $\text{O}_{6.4}$ sample shows the largest change in resistance ($\sim 37\%$) and 1.88-eV luminescence ($\sim 15\%$) upon 4-W illumination, the $\text{O}_{6.6}$ sample shows smaller decreases in resistivity ($\sim 19\%$) and 1.88-eV luminescence ($\sim 6\%$) and a small increase in the 2.4-eV luminescence. No perceptible change is observed in the resistance nor the luminescence spectra of the $\text{O}_{7-\delta}$ superconducting sample since there are no oxygen vacancies available to trap photogenerated electrons. Detailed studies of photoluminescence versus oxygen content will be reported elsewhere.

In proposing an oxygen-vacancy-defect-mediated mechanism for PPC and PISC in $\text{YBa}_2\text{Cu}_3\text{O}_{6+x}$, several pertinent issues need to be addressed: (1) Which of the observed luminescence peaks listed in Table I are defect-related, (2) where in the crystal are the electron-hole pairs photogenerated and where do they recombine, and (3) can the F center's stability account for the long observed decay times of the PPC-PISC effect?

For the first issue, it is beneficial to compare the peaks in the PISC efficiency as a function of excitation wavelength to the photoluminescence peaks listed in Table I (see Fig. 5). Figure 5 shows the numerical fit to the wavelength dependence of PPC (Refs. 2, 3) with the reported photoluminescence energy peaks indicated. There appears to be a strong correlation between the two spectra over the range of reported PPC efficiency data which suggest that both the luminescence spectrum and the PPC efficiency spectrum have a common origin. In our experiments, the peak at 2.03 eV does not change between the "unilluminated" and "photoinduced" states. This suggests that the 2.03-eV peak is not correlated to the PPC-PISC effect and is therefore not related to the defect mechanism. The broad luminescence feature near 2.4 eV may correspond, as it does in the PPC wavelength dependence (Fig. 5), to two overlapping photoluminescence peaks.

Unlike previous studies of the PPC mechanism which have suggested that the photogeneration of electron-hole

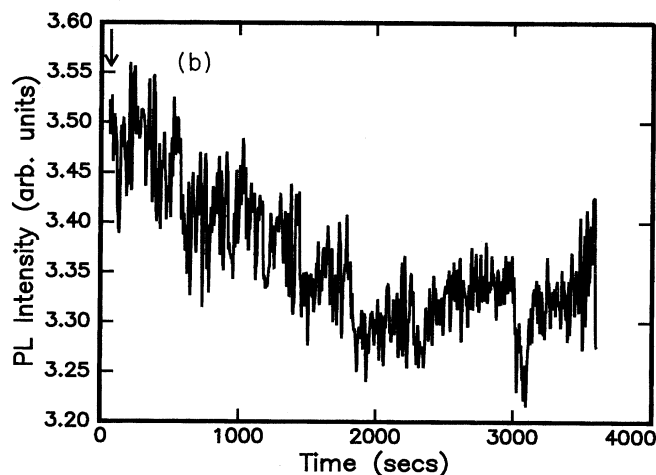
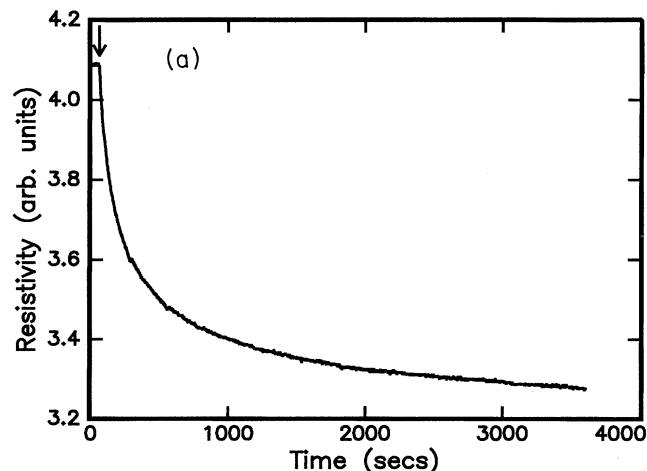


FIG. 4. (a) Resistivity and (b) 1.88-eV luminescence intensity during 4-W illumination of $\text{YBa}_2\text{Cu}_3\text{O}_{6.6}$. The arrows indicate when the sample is exposed to light.

pairs occurs in the CuO_2 plane, our results imply that both the photogeneration and luminescent recombination of electron-hole pairs occur in the Cu-O chain layer. In the charge-transfer model,² the photogenerated holes stay in the CuO_2 plane while the photogenerated electrons transfer to the chain layers. Based upon our results, the relevant defects for PPC cannot be located in the CuO_2 planes. Since photoluminescence as well as PISC persists *even for metallic films with a suppressed T_c* , defects must reside in the Cu-O chain layers so that trapped electrons are physically separated from holes in conducting CuO_2 planes. Otherwise, the close proximity of holes to trapped electrons would lead to recombination and a rapid quenching of the PPC-PISC state. For this reason, previous studies of luminescence in YBCO superconductors must be due to impurities rather than intrinsic defects.^{27,28,16} Moreover, the correlation of the PISC efficiency and photoluminescence spectra suggests that the photogeneration of carriers and their annihilation via luminescent recombination occur at the same location in the $\text{YBa}_2\text{Cu}_3\text{O}_{6+x}$ crystal. Optical reflectivity measurements of $\text{YBa}_2\text{Cu}_3\text{O}_{6+x}$ support the supposition that the defects and

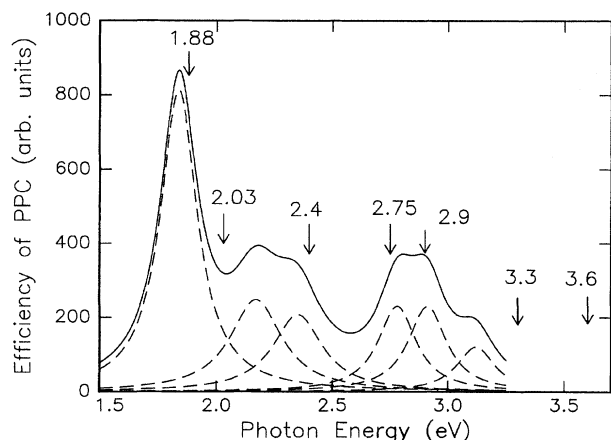


FIG. 5. Numerical fit to the wavelength dependence of PPC efficiency (Refs. 2, 3) (solid line). Individual Lorentz peaks are the dashed lines. Reported values of photoluminescence peaks (Table I) are indicated. The wavelength dependence of PPC reported in Refs. 2, 3 was limited by a range of 1.4–3.2 eV. The limited range might explain why the photoluminescent peak at 3.3 eV is displaced from the 3.1-eV PPC peak.

photogeneration of carriers occur in the chain layer. Optical studies of the a -, b -, and c -axis charge dynamics in $\text{YBa}_2\text{Cu}_3\text{O}_{6+x}$ reveal a 1.75-eV peak in the optical conductivity²⁹ which corresponds to charge transfer of a hole between the $\text{Cu}(2) d_{x^2-y^2}$ and $\text{O}(2,3) p_{x,y}$ sites on the CuO_2 planes. The absence of the 1.88-, 2.1-, 2.4-eV PPC features in optical reflectivity measurements of $\text{YBa}_2\text{Cu}_3\text{O}_{6+x}$ and Gd_2CuO_4 , which has no chain layers, implies that the spectral features observed in PPC and PISC and photoluminescence are *chain* excitations.

Since the PISC-PPC effect persists for hours at 77 K, the F center must be an extremely stable configuration. Two features stabilize the F center and prolong the lifetime of the photogenerated carriers: lattice deformation around the trapped electron and physical separation of the electrons and holes. Similar to other materials with F centers, one expects that the lattice locally deforms around the trapped electrons.

Lederman *et al.*⁶ report that upon photoexcitation of $\text{YBa}_2\text{Cu}_3\text{O}_{6+x}$, the lattice parameters shrink, indicating a more stable configuration. In addition, the large spatial separation between photogenerated electrons, which are trapped at oxygen vacancies in the CuO chain, and holes, which are in the conductive CuO_2 planes, implies a small overlap of their wave functions and therefore a lower probability for recombination of electrons and holes to quench the photoinduced conductivity.

In summary, photoconductivity and photoluminescence measurements on $\text{YBa}_2\text{Cu}_3\text{O}_{6+x}$ thin films strongly suggest a defect mechanism for persistent photoconductivity and photoinduced superconductivity in these materials. Oxygen vacancies in the Cu-O chains act as F centers which trap photogenerated electrons and prohibit their recombination with photogenerated holes. The correlation between the peaks observed in the luminescence spectra and those observed in the wavelength dependence of PPC suggest that the photogeneration of charges and their annihilation via luminescent recombination occur in the same location (Cu-O chains) of the $\text{YBa}_2\text{Cu}_3\text{O}_{6+x}$ crystal. Previous models had assigned the peaks in the PPC excitation spectrum to charge transfer in the CuO_2 planes. The defects which give rise to the PISC effect cannot be located in the CuO_2 planes since the large number of holes in the planes would easily annihilate the trapped electrons and quench the photoinduced state. In the oxygen vacancy defect model, the 1.88-eV level is assigned to the luminescence from electron-hole recombination at the defect site. The decrease in the 1.88-eV luminescence and increase in the 2.4-eV luminescence upon photoexcitation is a consequence of a decrease in the number of oxygen vacancies in the chain layers. The F center is stabilized by (1) lattice deformation around the captured electron and (2) physical separation of the trapped electron in the chain layer and the conducting hole in the plane layer.

This work was supported by the National Science Foundation and by Research Corporation. Helpful discussions with J. A. Joseph and L. Cooper are gratefully acknowledged. Sample packaging assistance by D. Brocking is acknowledged.

¹J. F. Federici, B. I. Greene, D. R. Dykaar, F. Sharifi, and R. C. Dynes, *Phys. Rev. B* **46**, 11 153 (1992).

²V. I. Kudinov, I. L. Chaplygin, A. I. Kirilyuk, N. M. Kreines, R. Laiho, E. Lahderanta, and C. Ayache, *Phys. Rev. B* **47**, 9017 (1993).

³S. L. Bud'ko, H. H. Feng, M. F. Davis, J. C. Wolfe, and P. H. Hor, *Phys. Rev. B* **48**, 16 707 (1993).

⁴G. Nieva, E. Osquiguil, J. Guimpel, M. Maenhoudt, B. Wuyts, Y. Bruynseraede, M. B. Maple, and Ivan K. Schuller, *Phys. Rev. B* **46**, 14 249 (1992).

⁵G. Yu, C. H. Lee, A. J. Heeger, N. Herron, E. M. McCarron, Lin Cong, G. C. Spalding, C. A. Nordman, and A. M. Goldman, *Phys. Rev. B* **45**, 4964 (1992).

⁶David Lederman, J. Hasen, Ivan K. Schuller, E. Osquiguil, and Y. Bruynseraede, *Appl. Phys. Lett.* **64**, 652 (1994).

⁷V. J. Emery and S. A. Kivelson, *Physica C* **209**, 597 (1993).

⁸V. I. Kudinov, A. I. Kirilyuk, N. M. Kreines, R. Laiho, and E. Lahderanta, *Phys. Lett. A* **151**, 358 (1990).

⁹V. I. Kudinov, I. L. Chaplygin, A. I. Kirilyuk, N. M. Kreines, R. Laiho, and E. Lahderanta, *Phys. Lett. A* **157**, 290 (1991).

¹⁰C. Ayache, I. L. Chaplygin, A. I. Kirilyuk, N. M. Kreines, and V. I. Kudinov, *Solid State Commun.* **81**, 41 (1992).

¹¹B. W. Veal, A. P. Paulikas, Hoydoo You, Hao Shi, Y. Fang, and J. W. Downey, *Phys. Rev. B* **42**, 6305 (1990).

¹²B. W. Veal, Hoydoo You, A. P. Paulikas, Hao Shi, Y. Fang, and J. W. Downey, *Phys. Rev. B* **42**, 4770 (1990).

¹³J. Hasen, David Lederman, Ivan K. Schuller, V. Kudinov, M. Maenhoudt, and Y. Bruynseraede, *Phys. Rev. B* **51**, 1342 (1995).

¹⁴J. F. Federici, D. Chew, B. Welker, W. Savin, T. Fink, and W. Wilber, *Bull. Am. Phys. Soc.* **40**, 742 (1995).

¹⁵M. Roth, A. Halperin, and S. Katz, *Solid State Commun.* **67**, 105 (1988).

- ¹⁶D. W. Cooke, M. S. Jahan, E. R. Gray, J. L. Smith, W. L. Hulst, B. L. Bennett, and M. A. Maez, *J. Lumin.* **48**, 819 (1991).
- ¹⁷Ch. B. Lushchik, I. L. Kussmann, E. Kh. Fel'dbakh, P. Kh. Liblik, T. I. Savikhina, and I. A. Meriloo, *Sov. Phys. Solid State* **29**, 2097 (1987).
- ¹⁸Ch. B. Lushchik, I. L. Kussmann, E. Kh. Fel'dbakh, K. E. Valaste, P. Kh. Liblik, A. A. Maaros, I. A. Meriloo, and T. I. Savikhina, *JETP Lett.* **46**, 151 (1987).
- ¹⁹I. Ya Fugol, V. N. Samovarov, Yu. I. Rybalko, and V. M. Zhuravlev, *Sov. J. Low Temp. Phys.* **16**, 337 (1990).
- ²⁰V. G. Stankevich, N. Yu. Svechnikov, K. V. Kaznacheev, R. A. Kink, I. L. Kuusmann, E. Kh. Feldbach, G. Zimmerer, T. Kloiber, A. A. Zhokhov, G. A. Emel'chenko, M. A. Kalyagin, and V. Ya Kosyev, *J. Lumin.* **48**, 845 (1991).
- ²¹V. G. Stankevich, N. Yu. Svechnikov, K. V. Kaznacheev, R. A. Kink, I. L. Kuusmann, E. Kh. Feldbach, G. Zimmerer, T. Kloiber, A. A. Zhokhov, G. A. Emel'chenko, M. A. Kalyagin, and V. Ya Kosyev, *Nucl. Instrum. Methods Phys. Res. A* **308**, 8193 (1991).
- ²²M. N. Popova, A. V. Puyats, M. E. Springis, and E. P. Khlybov, *JETP Lett.* **48**, 667 (1988).
- ²³V. V. Eremenko, I. Ya. Fugol', V. N. Samovarov, and V. M. Zhuravlev, *JETP Lett.* **47**, 619 (1988).
- ²⁴V. N. Andreev, B. P. Zakharchenya, S. E. Nikitin, F. A. Chudnovskii, E. B. Shadrin, and E. M. Sher, *JETP Lett.* **46**, 492 (1987).
- ²⁵B. J. Luff, P. D. Townsend, and J. Osbourne, *J. Phys. D* **21**, 663 (1988).
- ²⁶D. W. Cooke, H. Rempp, Z. Fisk, J. L. Smith, and M. S. Jahan, *Phys. Rev. B* **36**, 2287 (1987).
- ²⁷D. W. Cooke, M. S. Jahan, J. L. Smith, M. A. Maez, W. L. Hulst, I. D. Raistrick, D. E. Peterson, J. A. O'Rourke, S. A. Richardson, J. D. Doss, E. R. Gray, B. Rusnak, G. P. Lawrence, and C. Fortgang, *Appl. Phys. Lett.* **54**, 960 (1989).
- ²⁸D. W. Cooke, B. Bennett, E. R. Gray, R. J. Houlton, W. L. Hulst, M. A. Maez, A. Mayer, J. L. Smith, and M. S. Jahan, *Appl. Phys. Lett.* **55**, 1038 (1989).
- ²⁹S. L. Cooper, D. Reznik, A. Kotz, M. A. Karlow, R. Lui, M. V. Klein, W. C. Lee, J. Giapintzakis, D. M. Ginsberg, B. W. Veal, and A. P. Paulikas, *Phys. Rev. B* **47**, 8233 (1993).